

Surface Science Letters

Gas source homoepitaxy on Si(113) – the interrelation of H-induced reconstructions and growth morphology

V. Dorna *, Z. Wang ¹, U. Köhler*Institut für Experimentalphysik IV, AG Oberflächen, Ruhr-Universität Bochum, 44780 Bochum, Germany*

Received 10 November 1997; accepted for publication 12 January 1998

Abstract

High-temperature, time-lapsed STM-studies are used to investigate the surface morphology and the growth mode of gas source MBE of Si on Si(113) with disilane (Si_2H_6) as a precursor. A varying hydrogen coverage on the growing surface caused by the dynamic equilibrium between hydrogen supply from the precursor and thermal H desorption at 480°C results in several different reconstructions. Phases with (2×7) and (2×5) at a low flux of disilane and a (2×2) at high flux were distinguished that consist of only two basic elements: a low-H-coverage double-row structure and the gradual insertion of high-H-coverage (2×2) -like heavy domain walls. Above H coverages resulting in the (2×5) larger domains of (2×2) separate, for which a model is suggested. Besides an anisotropic shape of the Si islands in all stages of growth, a strong influence of the H-induced reconstructions on the silicon growth mode is found. Whereas step flow dominates for the lower H-coverage structure (2×7) and (2×5) , the formation of the (2×2) leads to a massive nucleation of Si islands arranged in a quasi-periodic way. This difference in nucleation behaviour results in a mechanism for a layer-by-layer-like growth mode, even on a surface with a very high hydrogen coverage in contrast to Si(111). © 1998 Elsevier Science B.V. All rights reserved.

Keywords: Chemical vapor deposition; Epitaxy; Growth; High index single crystal surfaces; Scanning tunneling microscopy; Silane; Silicon; Surface relaxation and reconstruction; Surface structure, morphology, roughness, and topography

Although silicon-based surface technology is still dominated by (001) and (111) surfaces, high indexed surfaces have also attracted increasing interest in the last years. In particular, the thermal stability of Si(113) has made it a possible candidate for future technological applications.

The structure of the clean Si(113) surface was investigated intensively by scanning tunnelling microscopy in recent years [1–3]. A (3×2) reconstruction with a high density of translational

domain walls was found to be the typical reconstruction at room temperature. A model by Dabrowski et al. [4] explains this reconstruction and the observed transition between the (3×2) and a (3×1) phase by a unit cell containing a subsurface self-interstitial. The surface energy that they calculated is small and close to the value for a hypothetical Si(001)-p(2×2) [4]. In X-ray scattering studies [5], however, only a (3×1) - and no evidence of a (3×2) reconstruction was found. Probably because of the small differences between both reconstructions, the X-ray structure factor of the (3×2) periodicity seems to be small compared to that resulting from the (3×1) periodicity. The calculated unit cell dimensions of this reconstruc-

* Corresponding author. Fax: (+49) 234 7094 173;
e-mail: volker.dorna@ep4-of.ruhr.uni

¹ Present address: Department of Applied Physics, Hunan University, People's Republic of China.

tion are 1.152 nm along $[\bar{1}10]$ and 0.637 nm along $[33\bar{2}]$.

Whereas the structure of the clean Si(113) seems to be resolved, little is known about the growth behaviour on this surface, even in homoepitaxy. In this context, the behaviour of hydrogen plays an important role because gas source MBE often involves H-containing precursors. However, in growth regimes where faceting on other Si surfaces occurs, quite often (113)-type faces appear as stable facets, i.e. in the case of the formation of 3d islands of Ge on Si [6] and especially during homoepitaxial growth under the influence of hydrogen [7]. The adsorption of hydrogen on Si(113) was found to proceed in two steps investigated by LEED, AES, ARUPS and HREELS [8–11]. During the first step, only Si–H bonds are formed, and the (3×2) turns into a (3×1) . In the second step, additionally, H–Si–H bonds are formed, and the reconstruction changes into (1×1) at a higher dosis. In contrast to these data, Wilson et al. [12] found, using STM studies, a mixture of (2×2) and (2×3) after exposure to atomic hydrogen at room temperature with no signs of (3×1) .

Although hydrogen adsorption on Si(113) was intensively studied, little has been published in context with epitaxial growth. On a low-index silicon surface, the detailed mechanism of the decomposition of disilane (Si_2H_6) used as a precursor gas is known. On Si(111), disilane decomposes above 420°C into 2SiH and $2\text{H}_2(\text{g})$ on the surface [13]. Above 500°C , two additional reaction paths, where Si and H are deposited as reaction products, have been identified [13,14]. Also, the morphology of the growing surface is known in the case of Si(111) and Si(001) [15].

The maximum of the hydrogen desorption peak on silicon is around 550°C . Therefore, we performed experiments on Si(113), especially between 420 and 550°C , to determine the correlation between the hydrogen-induced structure and the growth mode on this surface. In this temperature range, the competition between H supply by adsorption of disilane and thermal desorption leads to different hydrogen coverages, depending on the temperature and growth rate.

The experiments were performed in an ion-

pumped UHV chamber. Disilane was supplied through a standard UHV leak valve. The Si(113) wafers were outgassed at 600°C for 8 h and then flashed several times up to 1250°C . After the last flash, the samples were cooled down at a rate of 10°C s^{-1} .

The time-resolved STM measurements were performed in situ by taking snapshots of a selected surface area during epitaxial growth at elevated temperature. It has to be considered that the STM tip, depending on its geometrical form, may more or less shade the observed area and thus lower the effective pressure of the precursor in this area. For disilane, this effect is – for tips that are not too blunt – negligible. Because of the low sticking coefficient of about 1×10^{-3} ([16] on Si(111)) the molecules can diffuse underneath the tip using multiple collisions. Nevertheless, the features seen in in-situ STM observations were compared with images that were obtained without the presence of a tip during growth to exclude tip-induced effects on the growth process. All STM images shown in this paper were obtained in the constant current mode at 0.5 nA and a sample bias U_B of -2 V.

After preparation in UHV, the clean Si(113) surface shows a (3×2) reconstruction with a high density of anti-phase boundaries at room temperature (Fig. 1). The average miscut of the wafer

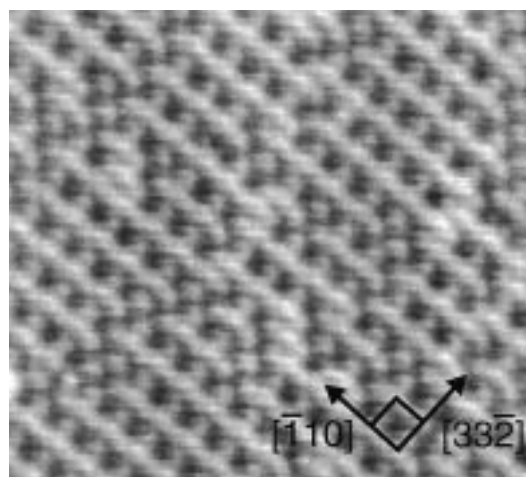


Fig. 1. Clean (3×2) -reconstructed Si(113) surface at room temperature with the typical high density of anti-phase boundaries walls ($U_B = -2$ V, 17×15 nm²).

used as a substrate was 0.2° , resulting in a typical terrace width of 100 nm.

If the samples are exposed to disilane at an elevated temperature and very low pressures in the range of 5×10^{-9} mbar, a (3×1) reconstruction becomes visible, which vanishes with increasing flux of disilane. This effect can be reversed by lowering the partial pressure. In contrast to the static adsorption of H at room temperature [8,9], the pressure dependence enables us to dynamically adjust the hydrogen coverage of the surface.

As on Si(111), no continuous growth could be observed below 420°C on (113). For an appreciable growth rate, the temperature has to be some 10°C above this threshold. For all temperatures between 450 and 550°C , we observed the same growth modes – in this range of temperature, the limiting process for the growth rate is the thermal desorption of hydrogen [17] as on Si(111) and Si(001). To concentrate on the disilane flux dependence in this paper, only in-situ measurements at 480°C are presented.

For the investigation of dynamic processes, time-resolved continuous scans of the same surface area were performed to obtain information on changes in surface morphology. In the course of an experiment, the disilane pressure was increased successively. Fig. 2 shows four selected images of such a sequence of STM scans, in which an overall view of a surface area can be seen. The time interval between the first and last frame is 44 min, the scanned area is $140 \times 140 \text{ nm}^2$.

In Fig. 2a, several terraces separated by mono- or diatomic steps are visible. The image was taken at a partial pressure of 1.2×10^{-8} mbar. At such a low flux of disilane, diffusion of adsorbed species leads to a final accommodation of silicon only at the step edges. Step flow perpendicular to the step edges is predominant, but already a restructuring of the steps takes place. The step edges consist of smooth sections parallel and rough sections perpendicular to the $[\bar{1}10]$ direction. The $[\bar{1}10]$ and $[3\bar{3}\bar{2}]$ directions, which are parallel and perpendicular to the dimers in the (3×1) reconstruction, are marked in Fig. 2a.

Fig. 2b shows the same surface area, after the partial pressure was increased to 4.0×10^{-6} mbar. Although growth still proceeds at step edges, the

surface structures become increasingly anisotropic. As Fig. 2c shows, a further increase in disilane pressure (8.5×10^{-6}) intensifies this effect. At this moderate flux of disilane, the effective diffusion length of the adsorbed species along $[\bar{1}10]$ is still in the order of the terrace width of the investigated samples, and step flow is dominant, although some string-shaped islands along the $[\bar{1}10]$ direction with a length of 100 nm and a width of several nanometres are seen. A surface reconstruction, visible as streaks along the $[\bar{1}10]$ direction, which could not be observed at lower pressures, is accompanied by this growth mode. This will be investigated in further detail below.

The size of the surface structures decreases further with increasing disilane pressure, and finally at pressures above 2×10^{-5} mbar, a massive formation of islands takes place, which are also characterized by their strong anisotropy. At 3.7×10^{-5} mbar (Fig. 2d), the typical length of these islands along the $[\bar{1}10]$ direction is 10 nm, whereas their width is only several angstroms. A quasi-periodical arrangement of these islands perpendicular to the $[\bar{1}10]$ direction can be observed (see below).

A 20-min exposure at a disilane pressure of 2×10^{-4} reduces the length of the nucleated islands, but no roughening of the surface was observed. This may be a sign that the growth is in a state of equilibrium, and no faceting – in contrast to the Si(111) surface [7,13] – takes place. After quenching the disilane partial pressure, the islands dissolve again, and the obtained images are similar to Fig. 2a.

To better resolve the different atomic arrangements in the different stages of growth, “zoomed-in scans” with an atomic resolution area of $15 \times 15 \text{ nm}^2$ are shown in Fig. 3. A structure with a (2×7) reconstruction is obtained at a pressure of 6.5×10^{-6} mbar (Fig. 3a) that contains two structural elements, one part consisting of three rows along $[\bar{1}10]$, each row with a width of two unit cells and a “double chain”-like structure (marked with \circ) and another row with clearly visible protrusions (marked with \triangle). The twofold periodicity of both parts along $[\bar{1}10]$ in the unit cell can be understood as being a consequence of the dimerization within the (001)-like Si-sites of

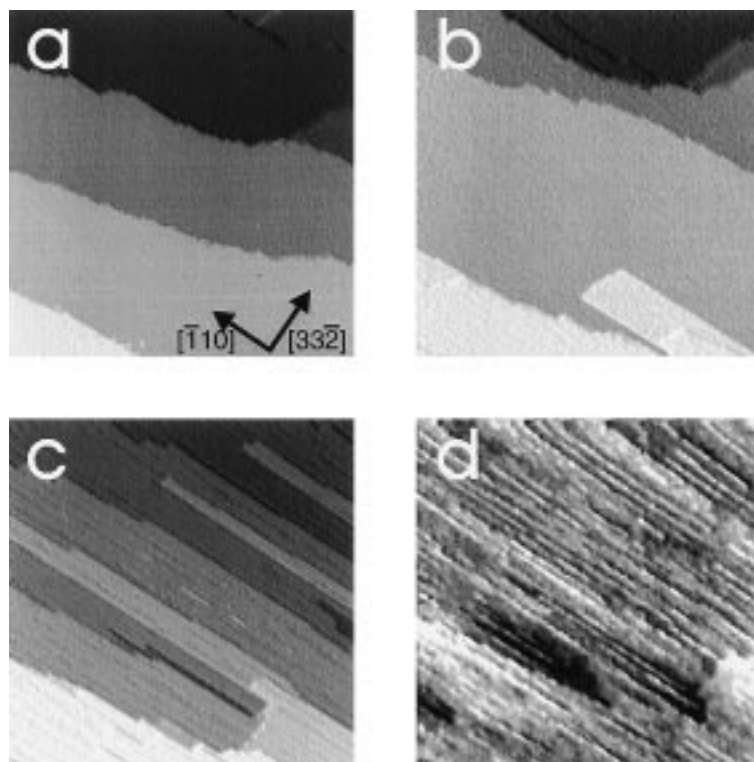


Fig. 2. Selected frames of a time-lapsed sequence of STM images ($140 \times 140 \text{ nm}^2$) giving an overview of the morphology during growth. The scans show the same surface area during deposition of silicon from disilane at 480°C . With increasing flux of disilane, the step flow turns into an asymmetric restructuring of step edges (b, c) and the nucleation of quasi-periodically arranged islands (d). The corresponding disilane partial pressures are (a) 1.2×10^{-8} , (b) 4.0×10^{-6} , (c) 8.5×10^{-6} , and (d) 3.7×10^{-5} mbar.

the bulk truncated surface consisting of (111)- and (001)-like sites alternating along $[33\bar{2}]$ (see below).

Let us first concentrate on the second structure element (Δ) that was found to dominate at a higher disilane flux forming a (2×2) reconstruction with a unit cell of $0.68 \times 1.25 \text{ nm}^2$, indicated in Fig. 3d at a corresponding pressure of 1.8×10^{-5} mbar.

We propose a structural model for this reconstruction as shown in Fig. 4. The (2×2) unit cell consists of a threefold coordinated ((111)-like) site and a tetramer containing a (001)-like dimer along $[\bar{1}10]$ and has eight dangling bonds for possible hydrogen adsorption. The structural elements are the same as in the model proposed by Wilson et al. [12], obtained from a STM study of H adsorption at 380°C ; only the symmetry of the unit cell is different. Whereas Wilson et al. propose a rectangular unit cell, our data show that the dimers in

subsequent rows are shifted with respect to each other resulting in a non-rectangular unit cell with an angle of 73° (see Fig. 4). Whereas our model reflects the correct symmetry of the unit cell, the protrusions visible in the STM images (e.g. Fig. 3d) are stretched along $[33\bar{2}]$, which means perpendicular to the direction of the (001)-like dimers. Further STM measurements and calculated STM images of the structural model together with the information about the locations of hydrogen are needed to determine which structural elements are visible in the filled state images. We did not observe an ordered structure different from (2×2) even at a higher flux, and we especially did not observe a (1×1) . In these terms, the (2×2) structure is the upper limit in hydrogen coverage during Si homoeptaxy with disilane as a precursor.

Returning to Fig. 3a, the surface structure can then be assigned as a reconstruction with a lower

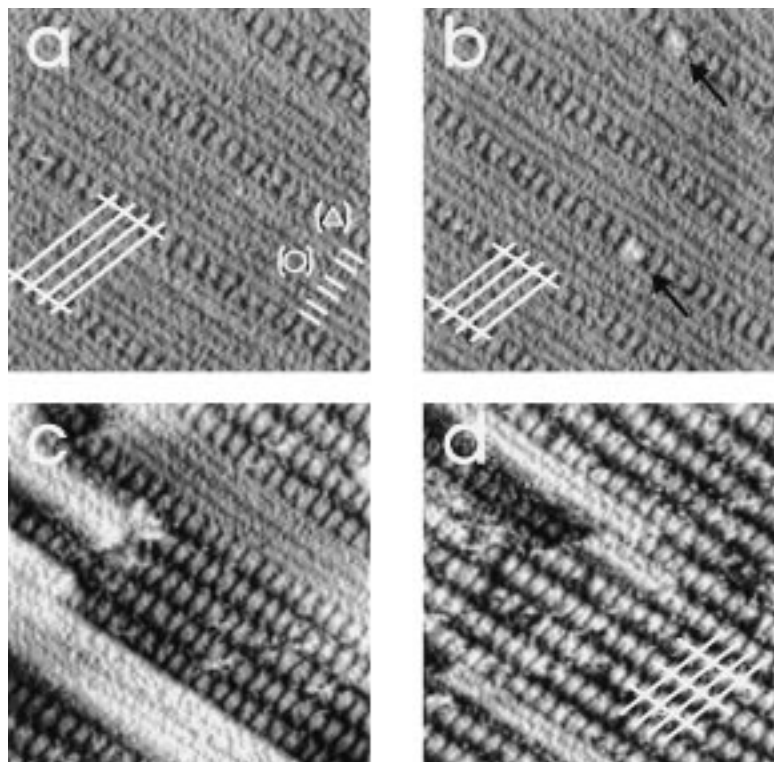


Fig. 3. Scans at increasing disilane flux with atomic resolution ($15 \times 15 \text{ nm}^2$, $U_B = -2 \text{ V}$). (a, b) Low-coverage phase with (2×7) - and (2×5) reconstructions at 6.5×10^{-6} and 7.5×10^{-6} mbar disilane partial pressure, (c) transition from (2×5) to (2×2) reconstruction (9.5×10^{-6} mbar) with nucleated islands, and (d) high-coverage phase with (2×2) reconstruction at 1.8×10^{-5} mbar. The images are high-pass filtered.

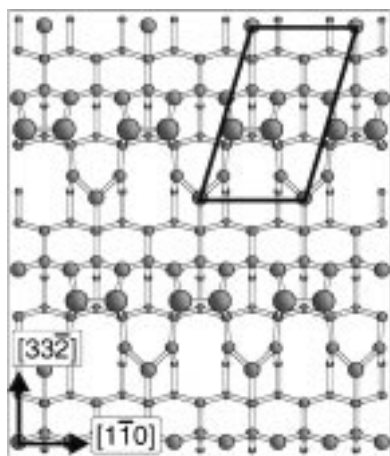


Fig. 4. Structural model for the high-coverage phase. The unit-cell of the (2×2) reconstruction is marked (see text).

hydrogen coverage that consists of two coexisting phases, one row (half a unit cell) of the (2×2) -like high-coverage phase (Δ) and the “double chain” structure interpreted as a low-H-coverage structure (\circ). Other in-situ and ex-situ measurements (not shown here) indicate that the single chains in this “double chain” structure are not equivalent. One row appears to be higher and is shifted against the other along the $[\bar{1}10]$ direction and both have a poorly visible twofold periodicity along $[\bar{1}10]$. However, these data are not sufficient for a structure model as yet.

Back to the course of the experiment, where we gradually increase the flux of disilane. In addition to the atomic details visible in Fig. 3, the development of the overall morphology of the domain structure is shown in Fig. 5.

A carefully increased disilane flux (Fig. 3b)

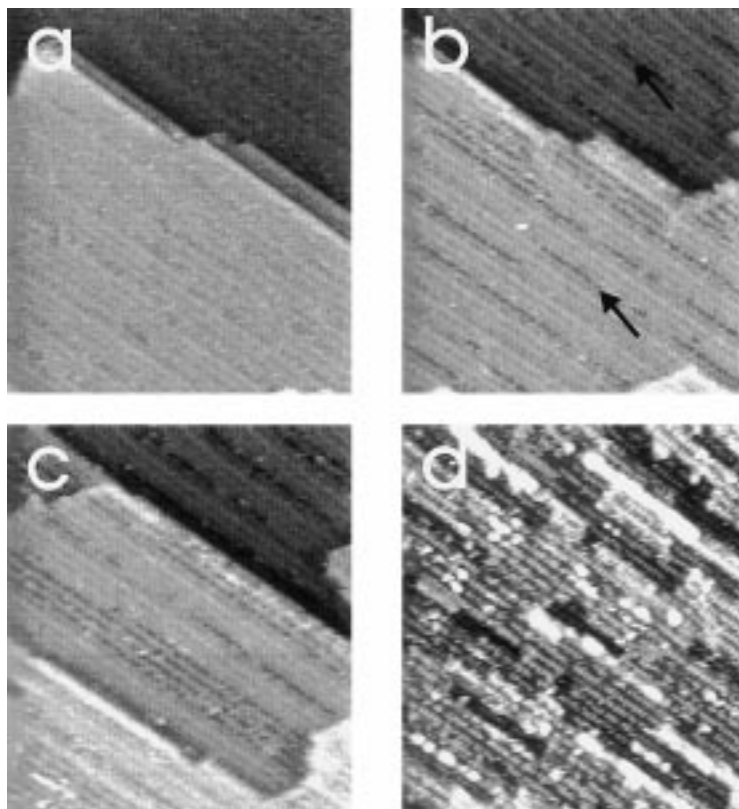


Fig. 5. Rearrangement of the surface reconstruction on a larger scale with increasing disilane flux ($40 \times 40 \text{ nm}^2$). (a) Restructuring of the surface at low flux, (b) insertion of high-coverage domain walls with (2×2) resulting in a (2×5) reconstruction, (c) (2×2) domains in coexistence with the low-H-coverage phase, (d) high-H-coverage phase with (2×2) reconstruction with a small fraction of nucleated islands. The corresponding disilane partial pressures are (a) 2.0×10^{-6} , (b) 8.2×10^{-6} , (c) 9.4×10^{-6} , and (d) 3.0×10^{-5} mbar.

changes the (2×7) into a (2×5) surface reconstruction with two, instead of three, low-coverage “double chains” in between the high-coverage rows. The alternation between high- and low-hydrogen-coverage structures can be interpreted as a domain wall structure with a striped symmetry, where the (2×2) -like rows depict heavy domain walls. At a higher flux of Si_2H_6 and therefore increasing H coverage, the separation of these walls shrinks. On a larger scale, a statistical mixture of (2×5) and (2×7) is present (Fig. 5b), the average separation shifts continuously with increasing flux of disilane. At step edges already at very early stages, domains with local (2×2) appear.

Beyond the (2×5) , no continuous transition to

a high-coverage phase with decreasing distances between the heavy domain walls takes place. In particular, no (2×3) superstructure was observed in contrast to the case of hydrogen adsorption reported in Ref. [12]. This means that a single “double chain” is not stable. Instead, increasing the disilane flux further leads to the formation of extended (2×2) reconstructed surface areas, whereas the remaining part of the surface still shows the (2×5) – both phases coexist at the same flux (see Fig. 5c). Further increased flux leads to a mostly (2×2) reconstructed surface with only occasionally visible low-coverage “double chains” that then can be considered as light domain walls in a dense H- (2×2) (see the upper part of Fig. 3c). Finally, at the highest flux, the surface is com-

pletely covered with the (2×2) (see Figs. 3d and 5d).

A strong correlation between the hydrogen-induced reconstruction and the growth mode exists. The formation of separated Si islands during growth does not take place below a flux of about 9×10^{-6} mbar. In Fig. 3b, small clusters nucleate at the high-coverage domain walls, but they are only temporary stable and dissolve again. Only at a higher flux are island chains created (Fig. 3c), which again nucleate on the high-H-coverage (2×2) regions of the surface.

The preferential nucleation on areas covered by the high-coverage phase – the site selectivity – is probably the reason for the abrupt transition from step flow to island nucleation, if the surface reconstruction changes in this pressure range as seen in Fig. 2c–d.

On top of the nucleated islands, the reconstruction differs from the underlying (2×2) and has initially the same “double chain” structure as found in the low-H-coverage regions at a lower flux in Fig. 3a,b. The width of the islands depends dynamically on the actual flux; increasing the disilane partial pressure leads to narrower islands. Finally, the islands consist of only one “double chain” of the low H-coverage structure. On a perfect (2×2) -reconstructed surface, the observed islands show a quasi-periodical arrangement with a fourfold periodicity along [332], which means that every second row of the (2×2) is occupied by an island (see bottom right part of Fig. 5d).

The mode of continuous growth at a high disilane flux is dominated by the difference in nucleation rate on the (2×2) and on the islands showing the low-H-coverage structure. The growth of a new layer can be divided into two steps: on a completely (2×2) -reconstructed surface, islands nucleate with the low-H-coverage structure on top. Because the nucleation on these islands is strongly hindered, half a monolayer is formed in a near-perfect layer-by-layer growth mode until a periodic arrangement of islands is formed (see Fig. 2d). Only in the second step, when the islands coalesce, does the reconstruction gradually change to high-H-coverage (2×2) . In this way, the nucleation of the next layer is suppressed until approximately 0.75 of a complete layer has grown, and a layer-

by-layer growth mode is strongly favoured, even at a very high growth rate, where the surface is largely hydrogen-covered.

The interplay of hydrogen-induced reconstructions and nucleation behaviour of new islands therefore prevents a roughening of the (113) surface at a high flux of disilane in contrast to Si(111). This high stability of Si(113) during growth may make this surface orientation an interesting candidate for technological applications. Heteroepitaxy on Si(113) and the influence of typical surfactants like Sb [18] are presently investigated and will be of future interest.

In conclusion, it was possible to show that the morphology and the growth mode of gas source MBE-grown Si on Si(113) are strongly driven by the observed H-induced surface reconstructions, which are different to those obtained by adsorption of atomic hydrogen. Using high-temperature, time-lapsed STM “movies”, real space information on growth processes can be obtained in a very efficient and reliable manner.

Acknowledgements

We like to thank F. Meyer zu Heringdorf and H.J. Günter (Universität Hannover) for helpful discussions and the Volkswagenstiftung for financial support.

References

- [1] J. Knall, J.B. Pethica, J.D. Todd, J.H. Wilson, Phys. Rev. Lett. 66 (1991) 1733.
- [2] W. Arabczyk, S. Hinrich, H.J. Müssig, Vacuum 46 (1995) 473.
- [3] H. Sakama, D. Kunitatsu et al., Phys. Rev. B 53 (1996) 6927.
- [4] J. Dabrowski, H.J. Müssig, G. Wolff, Phys. Rev. Lett. 73 (1994) 1660.
- [5] S. Song, S.G.J. Mochrie, Phys. Rev. B 51 (1995) 10068.
- [6] U. Köhler, O. Jasko, G. Pietsch, B. Müller, M. Henzler, Surf. Sci. 248 (1991) 321.
- [7] U. Köhler, L. Andersohn, H. Bethge, Phys. Stat. Sol. (a) 159 (1997) 39.
- [8] U. Myler, P. Althainz, K. Jacobi, Surf. Sci. 251252 (1991) 607.
- [9] K. Jacobi, U. Myler, Surf. Sci. 284 (1993) 223.

- [10] H. Huang, S.Y. Tong, U. Myler, K. Jacobi, *Surf. Rev. Lett.* 1 (2)3 (1994) 221.
- [11] S.M. Scholz, K. Jacobi, *Phys. Rev. B* 52 (1995) 5795.
- [12] J.H. Wilson, P.D. Scott, J.B. Pethica, J. Knall, *J. Phys. Cond. Mat.* 3 (1991) 133.
- [13] U. Köhler, L. Andersohn, B. Dahlheimer, *Appl. Phys. A* 57 (1993) 491.
- [14] S.K. Kulkarni, S.M. Gates et al., *J. Vac. Sci. Technol. A* 8 (1990) 2956.
- [15] R.J. Hamers, U.K. Köhler, J.E. Demuth, *J. Vac. Sci. Technol. A* 8 (1990) 195.
- [16] L. Andersohn, T. Berke, U. Köhler, B. Voigtländer, *J. Vac. Sci. Technol. A* 14 (1996) 312.
- [17] F. Meyer zu Heringdorf, to be published.
- [18] H.J. Müssig, J. Dabrowski et al., *J. Vac. Sci. Technol. B* 14 (1996) 982.